

---

# On Sequential Bayesian Inference for Continual Learning

**Samuel Kessler**  
*University of Oxford*

*skessler@robots.ox.ac.uk*

**Adam Cobb**  
*SRI International*

*adam.cobb@sri.com*

**Tim G. J. Rudner**  
*University of Oxford*

*tim.rudner@cs.ox.ac.uk*

**Stefan Zohren**  
*University of Oxford*

*zohren@robots.ox.ac.uk*

**Stephen J. Roberts**  
*University of Oxford*

*sjrob@robots.ox.ac.uk*

## Abstract

Sequential Bayesian inference can be used for *continual learning* to prevent catastrophic forgetting of past tasks and provide an informative prior when learning new tasks. We revisit sequential Bayesian inference and test whether having access to the true posterior is guaranteed to prevent catastrophic forgetting in Bayesian neural networks. To do this we perform sequential Bayesian inference using Hamiltonian Monte Carlo. We propagate the posterior as a prior for new tasks by fitting a density estimator on Hamiltonian Monte Carlo samples. We find that this approach fails to prevent catastrophic forgetting demonstrating the difficulty in performing sequential Bayesian inference in neural networks. From there we study simple analytical examples of sequential Bayesian inference and CL and highlight the issue of model misspecification which can lead to sub-optimal continual learning performance despite exact inference. Furthermore, we discuss how task data imbalances can cause forgetting. From these limitations, we argue that we need probabilistic models of the continual learning generative process rather than relying on sequential Bayesian inference over Bayesian neural network weights. In this vein, we also propose a simple baseline called *Prototypical Bayesian Continual Learning*, which is competitive with state-of-the-art Bayesian continual learning methods on class incremental continual learning vision benchmarks.

## 1 Introduction

The goal of continual learning (CL) is to find a predictor that learns to solve a sequence of new tasks without losing the ability to solve previously learned tasks. One key challenge of CL with neural networks (NNs) is that model parameters from previously learned tasks are “overwritten” during gradient-based learning of new tasks, which leads to *catastrophic forgetting* of previously learned abilities (French, 1999). One approach to CL hinges on using recursive applications of Bayes’ Theorem; using the weight posterior in a Bayesian neural network (BNN) as the prior for a new task (Kirkpatrick et al., 2017). However, obtaining a full posterior over NN weights is computationally demanding and we often need to resort to approximations, such as the Laplace method (MacKay, 1992) or variational inference (Graves, 2011; Blundell et al., 2015) to obtain a neural network weight posterior.

When performing Bayesian CL, sequential Bayesian inference is performed with an approximate BNN posterior, not the true posterior (Schwarz et al., 2018; Ritter et al., 2018; Nguyen et al., 2017; Ebrahimi et al., 2019; Kessler et al., 2019; Loo et al., 2020). If we consider the performance of sequential Bayesian inference

---

with a variational approximation over a BNN weight posterior then we barely observe an improvement over simply learning new tasks with stochastic gradient descent (SGD). We will develop this statement further in Section 2.2. So if we had access to the true BNN weight posterior, would this be enough to prevent forgetting by sequential Bayesian inference?

Our contributions in this paper are to revisit Bayesian CL. 1) Experimentally, we perform sequential Bayesian inference using the true Bayesian NN weight posterior. We do this by using the gold standard of Bayesian inference methods, Hamiltonian Monte Carlo (HMC) (Neal et al., 2011). We use density estimation over HMC samples and use this approximate posterior density as a prior for the next task within the HMC sampling process. Surprisingly our HMC method for CL yields no noticeable benefits over an approximate inference method (VCL Nguyen et al. (2017)) despite using samples from the true posterior. 2) As a result we consider a simple analytical example and highlight that exact inference with a misspecified model can still cause forgetting. 3) We show mathematically that under certain assumptions task data imbalances will cause forgetting in Bayesian NNs. 4) We propose a new probabilistic model for CL and show that by explicitly modeling the generative process of the data, we can achieve good performance, avoiding the need to rely on recursive Bayesian inference over NN weights to prevent forgetting. Our proposed model, *Prototypical Bayesian Continual Learning* (ProtoCL), is conceptually simple, scalable, and competitive with state of the art Bayesian CL methods in the class-incremental learning setting.

## 2 Background

### 2.1 The Continual Learning Problem

*Continual learning* (CL) is a learning setting whereby a model must learn to make predictions over a set of tasks sequentially while maintaining performance across all previously learned tasks. In CL, the model is sequentially shown  $T$  tasks, denoted  $\mathcal{T}_t$  for  $t = 1, \dots, T$ . Each task,  $\mathcal{T}_t$ , is comprised of a dataset  $\mathcal{D}_t = \{(\mathbf{x}_i, y_i)\}_{i=1}^{N_t}$  which a model needs to learn to make predictions with. More generally, tasks are denoted by distinct tuples comprised of the conditional and marginal data distributions,  $\{p_t(y|\mathbf{x}), p_t(\mathbf{x})\}$ . After task  $\mathcal{T}_t$  the model will lose access to the training dataset but its performance will be continually evaluated on all tasks  $\mathcal{T}_i$  for  $i \leq t$ . For a comprehensive review of CL scenarios see (Hsu et al., 2018; Van de Ven & Tolias, 2019). We decompose predictors as  $g = h \circ f$  such that  $\hat{y} = g(\mathbf{x})$  we define  $f$  as an embedding function mapping  $f: \mathcal{X} \rightarrow \mathcal{Z}$  and  $h$  as a head mapping to outputs  $h: \mathcal{Z} \rightarrow \mathcal{Y}$ . Some continual learning methods use a separate head per task  $\{h_i\}_{i=1}^T$ , these methods are called multi-headed while those that use one head are called single-headed.

### 2.2 Bayesian Continual Learning

We consider a setting in which task data arrives sequentially at time steps,  $t = 1, 2, \dots, T$ . At the first time step,  $t = 1$ , the model parameterized by  $\boldsymbol{\theta}$  receives the dataset  $\mathcal{D}_1$  and learns the conditional distribution  $p(y_i|\mathbf{x}_i, \boldsymbol{\theta})$  for all  $(\mathbf{x}_i, y_i) \in \mathcal{D}_1$  ( $i$  indexes a datapoint), the parameters  $\boldsymbol{\theta}$  have a prior distribution  $p(\boldsymbol{\theta})$ . The posterior predictive distribution for a test point,  $\mathbf{x}_1^*$  is:

$$p(y_1^*|\mathbf{x}_1^*, \mathcal{D}_1) = \int p(y_1^*|\mathbf{x}_1^*, \boldsymbol{\theta})p(\boldsymbol{\theta}|\mathcal{D}_1)d\boldsymbol{\theta}. \quad (1)$$

Computing this posterior predictive distribution above requires  $p(\boldsymbol{\theta}|\mathcal{D}_1)$ . For  $t = 2$ , a CL model is required to fit  $p(y_i|\mathbf{x}_i, \boldsymbol{\theta})$  for  $\mathcal{D}_1 \cup \mathcal{D}_2$ . The posterior predictive distribution for a new test point  $\mathbf{x}_2^*$  point is:

$$p(y_2^*|\mathbf{x}_2^*, \mathcal{D}_1, \mathcal{D}_2) = \int p(y_2^*|\mathbf{x}_2^*, \boldsymbol{\theta})p(\boldsymbol{\theta}|\mathcal{D}_1, \mathcal{D}_2)d\boldsymbol{\theta}. \quad (2)$$

The posterior must thus be updated to reflect this new conditional distribution. We can use repeated application of Bayes' rule to calculate the posterior distributions  $p(\boldsymbol{\theta}|\mathcal{D}_1, \dots, \mathcal{D}_T)$  as:

$$p(\boldsymbol{\theta}|\mathcal{D}_1, \dots, \mathcal{D}_{T-1}, \mathcal{D}_T) = \frac{p(\mathcal{D}_T|\boldsymbol{\theta})p(\boldsymbol{\theta}|\mathcal{D}_1, \dots, \mathcal{D}_{T-1})}{p(\mathcal{D}_T|\mathcal{D}_1, \dots, \mathcal{D}_{T-1})}. \quad (3)$$

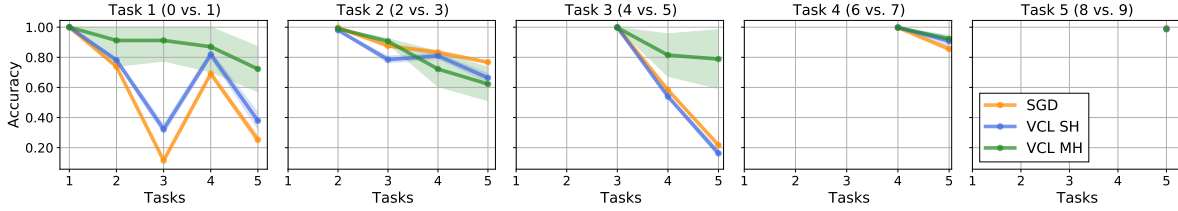


Figure 1: Accuracy on Split-MNIST for various CL methods with a two-layer BNN. We compare a NN trained with SGD (single-headed) with VCL. We consider single-headed (SH) and multi-head (MH) VCL variants.

In the CL setting we lose access to previous training datasets: however, using repeated applications of Bayes' rule Eq. (3), allows us to sequentially incorporate information from past tasks in the parameters  $\theta$ . At  $t = 1$ , we have access to  $\mathcal{D}_1$  and the posterior over weights is:

$$\log p(\theta|\mathcal{D}_1) = \log p(\mathcal{D}_1|\theta) + \log p(\theta) - \log p(\mathcal{D}_1). \quad (4)$$

At  $t = 2$ , we require a posterior  $p(\theta|\mathcal{D}_1, \mathcal{D}_2)$  to calculate the posterior predictive distribution in Eq. (2). However, we have lost access to  $\mathcal{D}_1$ . According to Bayes' rule, the posterior may be written as:

$$\log p(\theta|\mathcal{D}_1, \mathcal{D}_2) = \log p(\mathcal{D}_2|\theta) + \log p(\theta|\mathcal{D}_1) - \log p(\mathcal{D}_2|\mathcal{D}_1), \quad (5)$$

where we used the conditional independence of  $\mathcal{D}_2$  and  $\mathcal{D}_1$  given  $\theta$ . We note that the likelihood is only dependent upon the current task dataset,  $\mathcal{D}_2$ , and that the prior encodes parameter knowledge from the previous task. Hence, we can use the posterior at  $t$  as a prior for learning a new task at  $t + 1$ . For the MNIST dataset (LeCun et al., 1998) we know that if we were to train a BNN we would achieve a good performance by inferring  $p(\theta|\mathcal{D})$ . Hence if we were to Split-MNIST into 5 two-way classification tasks then we should be able to recursively recover the multi-task posterior  $p(\theta|\mathcal{D}) = p(\theta|\mathcal{D}_1 \dots, \mathcal{D}_5)$ . This problem is called Split-MNIST. From Eq. (5) we require that our model with parameters  $\theta$  is a sufficient statistic of  $\mathcal{D}_1$ , making the likelihood conditionally independent of  $\mathcal{D}_1$  given  $\theta$ . This observation motivates the use of high-capacity predictors, such as Bayesian neural networks, that are flexible enough to learn  $\mathcal{D}_1$ .

### 2.3 Variational Continual Learning

Variational CL (VCL; Nguyen et al. (2017)) simplifies the Bayesian inference problem in Eq. (5) into a sequence of approximate Bayesian updates on the distribution over random neural network weights  $\theta$ . To do so, VCL uses the variational posterior from previous tasks as a prior for new tasks. In this way, learning to solve the first task entails finding a variational distribution  $q_1(\theta|\mathcal{D}_1)$  that maximizes a corresponding variational objective. For the subsequent task, the prior is chosen to be  $q_1(\theta|\mathcal{D}_1)$ , and the goal becomes to learn a variational distribution  $q_2(\theta|\mathcal{D}_2)$  that maximizes a corresponding variational objective under this prior. Denoting the recursive posterior inferred from multiple datasets by  $q_t(\theta|\mathcal{D}_{1:t})$ , we can express the variational CL objective for the  $t$ -th task as:

$$\mathcal{L}(\theta, \mathcal{D}_t) = \mathbb{D}_{\text{KL}}[q_t(\theta)||q_{t-1}(\theta|\mathcal{D}_{1:t-1})] - \mathbb{E}_{q_t}[\log p(\mathcal{D}_t|\theta)]. \quad (6)$$

When applying VCL to the problem of Split-MNIST Figure 1, we can see that single-headed VCL barely performs better than SGD when remembering past tasks. Multi-headed VCL performs better, despite not being a requirement from sequential Bayesian inference Eq. (5). So why does single-head VCL not improve over SGD if we can recursively build up an approximate posterior using Eq. (5)? We hypothesize that it could be due to using a variational approximation of the posterior and so we are not actually strictly performing the Bayesian CL process described in Section 2.2. We test this hypothesis in the next section by propagating the true BNN posterior to verify whether we can recursively obtain the true multi-task posterior and so improve on single-head VCL and prevent catastrophic forgetting.

### 3 Bayesian Continual Learning with Hamiltonian Monte Carlo

To perform inference over BNN weights we use the HMC algorithm (Neal et al., 2011). We then use these samples and learn a density estimator that can be used as a prior for a new task<sup>1</sup>. HMC is considered the gold standard in approximate inference and is guaranteed to asymptotically produce samples from the true posterior<sup>2</sup>. we use posterior samples of  $\theta$  from HMC and then fit a density estimator over these samples, to use as a prior for a new task. This allows us to use a multi-modal posterior distribution over  $\theta$ . In contrast, to a diagonal Gaussian variational posterior like in VCL. More concretely, to propagate the posterior  $p(\theta|\mathcal{D}_1)$  we use a density estimator, defined  $\hat{p}(\theta|\mathcal{D}_1)$ , to fit a probability density on HMC samples as a posterior. For the next task  $\mathcal{T}_2$  we can use  $\hat{p}(\theta|\mathcal{D}_1)$  as a prior for a new HMC sampling chain and so on (see Fig. 2). The density estimator priors need to satisfy two key conditions for use within HMC sampling. Firstly, that they are a probability density function. Secondly, that they are differentiable with respect to the input samples.

We use a toy dataset (Fig. 3) with two classes and inputs  $\mathbf{x} \in \mathbb{R}^2$  (Pan et al., 2020). Each task is a binary classification problem where the decision boundary extends from left to right for each new task. We train a two layer BNN, with hidden state size of 10. We use a Gaussian Mixture Models (GMM) as a density estimator for approximating the posterior with HMC samples. We also tried Normalizing Flows which should be more flexible (Dinh et al., 2016) however these did not work robustly for HMC sampling<sup>3</sup>. To the best of our knowledge we are the first to incorporate flexible priors into the sampling methods like HMC.

Training a BNN with HMC on the same multi-task dataset gets a test accuracy of 1.0. Thus, the final posterior is suitable for continual learning under Eq. (3) we should be able to recursively arrive at the multi-task posterior with our recursive inference method with HMC. The results from Fig. 3 demonstrate that using HMC with an approximate multi-modal posterior fails to prevent forgetting and is less effective than using multi-head VCL. In fact, multi-head VCL clearly outperforms HMC indicating that the source of the knowledge retention is not through the propagation of the posterior but through the task specific heads. We also repeated these experiments with another toy dataset of five binary classification tasks where we observe similar results (Fig. 7).

For HMC we ensure that we are sampling from the posterior by assessing chain convergence and effective sample sizes (Fig. 11). The effective sample size measures the autocorrelation in the chain. The effective sample sizes for the HMC chains for our BNNs are similar to the literature (Cobb & Jalaian, 2021). Also, we ensure that our GMM approximate posteriors are multi-modal and so has a more complex posterior in comparison to VCL, and that the GMM samples produce equivalent results to HMC samples for the current task (Fig. 10). See Appendix B for details.

We are not able to perform sequential Bayesian inference in BNNs despite using HMC which is considered the gold standard of Bayesian deep learning. HMC and density estimation with a GMM produces richer, accurate and multi-modal posteriors. Despite this we are still not able to sequentially build up the multi-task posterior or get much better results than an isotropic Gaussian posterior like single-head VCL. The weak

<sup>1</sup>We considered Sequential Monte Carlo, but it is unable to scale to the dimensions required for the NNs we consider (Chopin et al., 2020). HMC on the other hand has recently been successfully scaled to BNNs (Cobb & Jalaian, 2021; Izmailov et al., 2021).

<sup>2</sup>In the NeurIPS 2021 Bayesian Deep Learning Competition, the goal was to find an approximate inference method that is as “close” as possible to the posterior samples from HMC.

<sup>3</sup>RealNVP was very sensitive to the choice of random seed, the samples from the learned distribution did not give accurate predictions for the current task and led to numerical instabilities when used as a prior within HMC sampling.

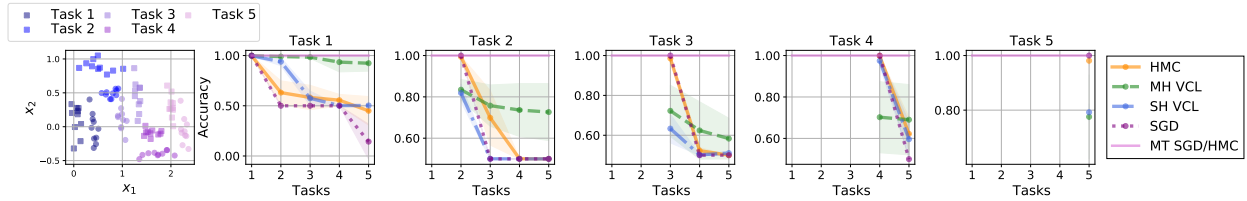


Figure 3: On the left is the toy dataset of 5 distinct 2-way classification tasks which involve classifying circles and squares (Pan et al., 2020). Also, continual learning binary classification test accuracies over 10 seeds. The pink solid line is a multi-task (MT) baseline accuracy using SGD/HMC with the same model as for the CL experiments.

point of this method is the density estimation, the GMM removes probability mass over areas of the BNN weight space posterior which is important for the new task. This demonstrates just how difficult a task it is to model BNN weight posteriors. In the next section, we study a different analytical example of sequential Bayesian inference and look at how model misspecification and task data imbalances can cause forgetting in Bayesian CL.

#### 4 Bayesian Continual Learning and Model Misspecification

We now consider a simple analytical example where we can perform the sequential Bayesian inference Eq. (3) in closed form using conjugacy. We consider a simple setting where data points arrive online, one after another.

Observations  $y_1, y_2, \dots, y_t$  arrive online, each observation is generated by a hidden variable  $\theta_1, \theta_2, \dots, \theta_t \sim p$  where  $p$  is a probability density function. At time  $t$  we wish to infer the *filtering distribution*  $p(\theta_t | y_1, y_2, \dots, y_t)$  (Doucet et al., 2001) using sequential Bayesian inference, similarly to the *Kalman filter* (Kalman, 1960). The likelihood is  $p(y_t | \theta_t) = \mathcal{N}(y_t; f(\cdot; \theta_t), \sigma^2)$  such that  $y_t = f(\cdot; \theta_t) + \epsilon$  where  $\epsilon \sim \mathcal{N}(0, \sigma^2)$  and  $f(\cdot; \theta_t) = \theta_t$ . We consider a Gaussian prior over the mean parameters  $\theta$  such that  $p(\theta_0) = \mathcal{N}(\theta_0; 0, \sigma_0^2)$ . Since the conjugate prior for the mean is also Gaussian, the prior and posterior are  $\mathcal{N}(\theta_{t-1}; \hat{\theta}_{t-1}, \hat{\sigma}_{t-1}^2)$  and  $\mathcal{N}(\theta_t; \hat{\theta}_t, \hat{\sigma}_t^2)$ . By using sequential Bayesian inference we can have closed-form update equations for our posterior parameters:

$$\hat{\theta}_t = \hat{\sigma}_t^2 \left( \frac{y_t}{\sigma^2} + \frac{\hat{\theta}_{t-1}}{\hat{\sigma}_{t-1}^2} \right) = \hat{\sigma}_t^2 \left( \sum_{i=1}^t \frac{y_i}{\sigma^2} + \frac{\hat{\theta}_0}{\hat{\sigma}_0^2} \right), \quad \frac{1}{\hat{\sigma}_t^2} = \frac{1}{\sigma^2} + \frac{1}{\hat{\sigma}_{t-1}^2}. \quad (7)$$

From Equation (7) the posterior mean follows a Gaussian distribution where the posterior mean is a sum of the online observation and the online prior. So the posterior mean is a weighted sum of the data. So, if the observations are non-stationary: if there is task change (more commonly referred to as a changepoint in the time-series literature). Then the mean parameter will encapsulate a global mean over both tasks rather than a mean for each task Fig. 4. The model is clearly misspecified since a single parameter cannot model both of these tasks together. *Despite performing exact inference a misspecified model can forget*, Fig. 4. In the case of HMC we verified that our Bayesian neural network had perfect performance on all tasks *beforehand*. In Section 3 we had a well specified model but struggled with exact sequential Bayesian inference Eq. (3). With this 1-d online learning scenario we are performing exact inference, however we have a misspecified model. It is important to disentangle model misspecification and exact inference, and highlight that model misspecification is a caveat which has not been highlighted in the CL literature as far as we are aware. Furthermore we can only ensure that our models are well specified if we have access to data from all tasks a

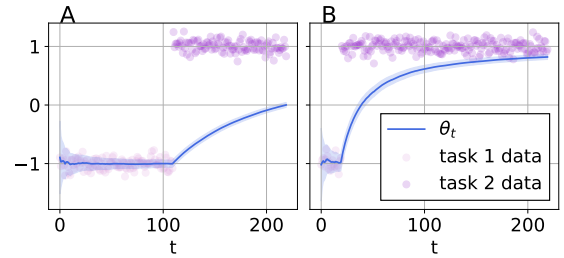


Figure 4: Posterior estimate of the filtering distribution Eq. (7) for two different scenarios with two tasks or changepoint.

priori. So in the scenario of *online continual learning* (De Lange et al., 2021) we cannot know if our model will perform well on all past and future tasks without making assumptions on the task distributions.

## 5 Sequential Bayesian Inference and Imbalanced Task Data

Neural Networks are complex models with a broad hypothesis space and hence are a suitably well-specified model when tackling continual learning problems (Wilson & Izmailov, 2020). However we struggle to fit the posterior samples from HMC to perform sequential Bayesian inference Section 3.

We continue to use Bayesian filtering and assume a Bayesian NN where the posterior is Gaussian with a full covariance. By modelling the entire covariance we enable modelling how each individual weight varies with respect to all others. We do this by interpreting online learning in Bayesian NNs as filtering (Ciftcioglu & Türkcan, 1995). Our treatment is similar to Aitchison (2018) who derives an optimizer by leveraging Bayesian filtering. We consider inference in the graphical model depicted in Fig. 5. The aim is to infer the optimal BNN weights,  $\theta_t^*$  at  $t$  given a single observation and the BNN weight prior. The previous BNN weights are used as a prior for inferring the posterior BNN parameters. We consider the online setting where a single data point  $(\mathbf{x}_t, y_t)$  is observed at a time.

Instead of modelling the full covariance we instead consider each parameter  $\theta_i$  as a function of all the other parameters  $\theta_{-it}$ . We also assume that the values of the weights are close to those of the previous timestep (Jacot et al., 2018). To obtain the update equations for BNN parameters given a new observation and prior we make two simplifying assumptions as follows.

**Assumption 5.1.** *For a Bayesian neural network with output  $f(\mathbf{x}_t; \boldsymbol{\theta})$  and likelihood  $\mathcal{L}(\mathbf{x}_t, y_t; \boldsymbol{\theta})$ , the derivative evaluated at  $\boldsymbol{\theta}_t$  is  $\mathbf{z}_t = \partial \mathcal{L}(\mathbf{x}_t, y_t; \boldsymbol{\theta}) / \partial \boldsymbol{\theta}|_{\boldsymbol{\theta}=\boldsymbol{\theta}_t}$  and the Hessian is  $\mathbf{H}$ . We assume a quadratic loss for a data point  $(\mathbf{x}_t, y_t)$  of the form:*

$$\mathcal{L}(\mathbf{x}_t, y_t; \boldsymbol{\theta}) = \mathcal{L}_t(\boldsymbol{\theta}) = -\frac{1}{2} \boldsymbol{\theta}^\top \mathbf{H} \boldsymbol{\theta} + \mathbf{z}_t^\top \boldsymbol{\theta}, \quad (8)$$

the result of a second-order Taylor expansion. The Hessian is assumed to be constant with respect to  $(\mathbf{x}_t, y_t)$  (but not with respect to  $\boldsymbol{\theta}$ ).

To construct the dynamical equation for  $\boldsymbol{\theta}$ , consider the gradient for the  $i$ -th weight while all other parameters are set to their current estimate at the optimal value for the  $\theta_{it}^*$ :

$$\theta_{it}^* = -\frac{1}{H_{ii}} \mathbf{H}_{-ii}^\top \boldsymbol{\theta}_{-it}, \quad (9)$$

since  $z_{it} = 0$  at a mode. The equation above shows us that the dynamics of the optimal weight  $\theta_{it}^*$  is dependent on all the other current values of the parameters  $\boldsymbol{\theta}_{-it}$ . The dynamics of  $\boldsymbol{\theta}_{-it}$  will be a complex stochastic process dependent on many different variables: such as the dataset, model architecture, learning rate schedule, etc.

**Assumption 5.2.** *Since reasoning about the dynamics of  $\boldsymbol{\theta}_{-it}$  are intractable, we assume that at the next time-step the optimal weights are close to the previous timesteps with a discretized Ornstein-Uhlenbeck process for the weights  $\boldsymbol{\theta}_{-it}$  with reversion speed  $\vartheta \in \mathbb{R}_+$  and noise variance  $\eta_{-i}^2$ :*

$$p(\boldsymbol{\theta}_{-i,t+1} | \boldsymbol{\theta}_{-i,t}) = \mathcal{N}((1 - \vartheta) \boldsymbol{\theta}_{-i,t}, \eta_{-i}^2), \quad (10)$$

this implies that the dynamics for the optimal weight is defined by

$$p(\theta_{i,t+1}^* | \theta_{i,t}^*) = \mathcal{N}((1 - \vartheta) \theta_{i,t}^*, \eta^2), \quad (11)$$

where  $\eta^2 = \eta_{-i}^2 \mathbf{H}_{-ii}^\top \mathbf{H}_{-ii}$ .

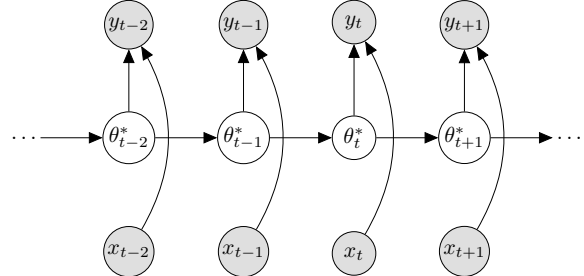


Figure 5: Graphical model for filtering. Grey and white nodes are observed and latent variables respectively.

In simple terms, in [Assumption 5.2](#) we assume a parsimonious model of the dynamics. That the next value of  $\theta_{-i,t}$  is close to their previous value according to a Gaussian, similarly to [Aitchison \(2018\)](#).

**Lemma 5.3.** *Under Assumptions 5.1 and 5.2 the dynamics and likelihood are Gaussian. Thus we are able to infer the posterior distribution over the optimal weights using Bayesian updates and by linearizing the BNN the update equations for the posterior of the mean and variance of the BNN for a new data point are:*

$$\mu_{t,post} = \sigma_{t,post}^2 \left( \frac{\mu_{t,prior}}{\sigma_{t,prior}^2(\eta^2)} + \frac{y_t}{\sigma^2} g(\mathbf{x}_t) \right) \quad \text{and} \quad \frac{1}{\sigma_{t,post}^2} = \frac{g(\mathbf{x}_t)^2}{\sigma^2} + \frac{1}{\sigma_{t,prior}^2(\eta^2)}, \quad (12)$$

where we drop the notation for the  $i$ -th parameter, the posterior is  $\mathcal{N}(\theta_t^*; \mu_{t,post}, \sigma_{t,post}^2)$  and  $g(\mathbf{x}_t) = \frac{\partial f(\mathbf{x}_t; \theta_{it}^*)}{\partial \theta_{it}^*}$  and  $\sigma_{t,prior}^2$  is a function of  $\eta^2$ .

See [Appendix E](#) for the derivation of [Lemma 5.3](#). From [Eq. \(12\)](#) we can notice that the posterior mean depends linearly on the prior and a data dependent term and so will behave similarly to our previous example in [Section 4](#). Under [Assumption 5.1](#) and [Assumption 5.2](#) then if there is a data imbalance between tasks in [Eq. \(12\)](#), then the data dependent term will dominate the prior term if there is more data for the current task.

In [Section 3](#) we showed that it is very difficult with current machine learning tools to perform sequential Bayesian inference for simple CL problems with small Bayesian NNs. When we disentangle Bayesian inference and model misspecification we show showed that misspecified models can forget despite exact Bayesian inference. The only way to ensure that our model is well specified is to show that the multi-task posterior produces reasonable posterior predictive distributions  $p(y|\mathbf{x}, \mathcal{D}) = \int p(y|\mathbf{x}, \mathcal{D}, \boldsymbol{\theta})p(\boldsymbol{\theta}|\mathcal{D})d\boldsymbol{\theta}$  for one's application. Additionally, in this section we have shown that if there is a task dataset size imbalance then we can get forgetting under certain assumptions.

## 6 Related Work

There has been a recent resurgence in the field of CL ([Thrun & Mitchell, 1995](#)) given the advent of deep learning. Methods which approximate sequential Bayesian inference [Eq. \(5\)](#) have been seminal in CL's revival and have used a diagonal Laplace approximation ([Kirkpatrick et al., 2017; Schwarz et al., 2018](#)). The diagonal Laplace approximation have been enhanced by modelling covariances of between neural network weights in the same layer ([Ritter et al., 2018](#)). Instead of the Laplace approximation we can use a variational approximation for sequential Bayesian inference ([Nguyen et al., 2017; Zeno et al., 2018](#)). Using richer priors has also been explored ([Ahn et al., 2019; Farquhar et al., 2020; Kessler et al., 2019; Mehta et al., 2021; Kumar et al., 2021; Loo et al., 2020](#)). Gaussian processes have also been applied to CL problems leveraging inducing points to retain previous task functions ([Titsias et al., 2019; Kapoor et al., 2021](#)).

Bayesian methods which regularize weights have not matched up to the performance of experience replay based CL methods ([Buzzega et al., 2020](#)) in terms of accuracy on CL image classification benchmarks. Instead of regularizing high dimension weight spaces, regularizing task functions is a more direct approach to combat forgetting ([Benjamin et al., 2018](#)). In particular, one can leverage the duality between the Laplace approximation and Gaussian Processes to develop a functional regularization approach to Bayesian CL ([Swaroop et al., 2019](#)) or using function-space variational inference ([Rudner et al., 2022a;b](#)).

## 7 Prototypical Bayesian Continual Learning

We have shown that sequential Bayes over NN parameters is very difficult ([Section 3](#)), and is only suitable for situations where the multi-task posterior is suitable for all tasks. We now show that a more fruitful approach is to model the full data-generating process of the CL problem and we propose a simple and scalable approach for doing so. In particular, we represent classes by prototypes ([Snell et al., 2017; Rebuffi et al., 2017](#)) to prevent catastrophic forgetting. We refer to this framework as Prototypical Bayesian Continual Learning, or ProtoCL for short. This approach can be viewed as a probabilistic variant of iCarl ([Rebuffi et al., 2017](#)), which creates embedding functions for different classes which are simply class means and predictions are

made by nearest neighbors. ProtoCL also bears similarities to the few-shot learning model Probabilistic Clustering for Online Classification (Harrison et al., 2019), developed for few-shot image classification.

**Model.** ProtoCL models the generative CL process. We consider classes  $j \in \{1, \dots, J\}$ , generated from a categorical distribution with a Dirichlet prior:

$$y_{i,t} \sim \text{Cat}(p_{1:J}), \quad p_{1:J} \sim \text{Dir}(\alpha_t). \quad (13)$$

Images are embedded into an embedding space by an encoder,  $\mathbf{z} = f(\mathbf{x}; \mathbf{w})$  with parameters  $\mathbf{w}$ . The per class embeddings are Gaussian whose mean has a prior which is also Gaussian:

$$\mathbf{z}_{it} | y_{it} \sim \mathcal{N}(\bar{\mathbf{z}}_{yt}, \Sigma_\epsilon), \quad \bar{\mathbf{z}}_{yt} \sim \mathcal{N}(\boldsymbol{\mu}_{yt}, \Lambda_{yt}^{-1}). \quad (14)$$

See Fig. 6 for an overview of the model. To alleviate forgetting in CL, ProtoCL uses a coreset of past task data to continue to embed past classes distinctly as prototypes. The posterior distribution over class probabilities  $\{p_j\}_{j=1}^J$  and class embeddings  $\{\bar{\mathbf{z}}_{y_j}\}_{j=1}^J$  is denoted in short hand as  $p(\boldsymbol{\theta})$  with parameters  $\eta_t = \{\alpha_t, \boldsymbol{\mu}_{1:J,t}, \Lambda_{1:J,t}^{-1}\}$ . ProtoCL models each class prototype but does not use task specific NN parameters or modules like multi-head VCL. By modeling a probabilistic model over an embedding space this allows us to use powerful embedding functions  $f(\cdot; \mathbf{w})$  without having to parameterize them probabilistically and so this approach will be more scalable than VCL, for instance.

**Inference.** As the Dirichlet prior is conjugate with the Categorical distribution and likewise the Gaussian over prototypes with a Gaussian prior over the prototype mean, we can calculate posteriors in closed form and update the parameters  $\eta_t$  as new data is observed without using gradient based updates. We optimize the model by maximizing the posterior predictive distribution and use a softmax over class probabilities to perform predictions. We perform gradient-based learning of the NN embedding function  $f(\cdot; \mathbf{w})$  and update the parameters,  $\eta_t$  at each iteration of gradient descent as well, see Algorithm 1.

**Sequential updates.** We can obtain our parameter updates for the Dirichlet posterior by Categorical-Dirichlet conjugacy:

$$\alpha_{t+1,j} = \alpha_{t,j} + \sum_{i=1}^{N_t} \mathbb{I}(y_t^i = j), \quad (15)$$

where  $N_t$  are the number of points seen during the update at time step  $t$ . Also, due to Gaussian-Gaussian conjugacy the posterior for the Gaussian prototypes is governed by:

$$\Lambda_{y_{t+1}} = \Lambda_{y_t} + N_y \Sigma_\epsilon^{-1} \quad (16)$$

$$\Lambda_{y_{t+1}} \boldsymbol{\mu}_{y_{t+1}} = N_y \Sigma_\epsilon^{-1} \bar{\mathbf{z}}_{y_t} + \Lambda_{y_t} \boldsymbol{\mu}_{y_t}, \quad \forall y_t \in C_t, \quad (17)$$

where  $N_y$  are the number of samples of class  $y$  and  $\bar{\mathbf{z}}_{y_t} = (1/N_y) \sum_{i=1}^{N_y} \mathbf{z}_{y_t}$ , see Appendix D.2 for the detailed derivation.

**Objective.** We optimize the posterior predictive distribution of the prototypes and classes:

$$p(\mathbf{z}, y) = \int p(\mathbf{z}, y | \boldsymbol{\theta}_t; \eta_t) p(\boldsymbol{\theta}_t; \eta_t) d\boldsymbol{\theta}_t = p(y) \prod_{i=1}^{N_t} \mathcal{N}(\mathbf{z}_{it} | y_{it}; \boldsymbol{\mu}_{y_t,t}, \Sigma_\epsilon + \Lambda_{y_t,t}^{-1}). \quad (18)$$

---

**Algorithm 1** ProtoCL continual learning

---

```

1: Input: task datasets  $\mathcal{T}_{1:T}$ , initialize embedding function:  $f(\cdot; \mathbf{w})$ , coresset:  $\mathcal{M} = \emptyset$ .
2: for  $\mathcal{T}_1$  to  $\mathcal{T}_T$  do
3:   for each batch in  $\mathcal{T}_i \cup \mathcal{M}$  do
4:     Optimize  $f(\cdot; \mathbf{w})$  by maximizing the posterior predictive  $p(\mathbf{z}, y)$  Eq. (18)
5:     Obtain posterior over  $\boldsymbol{\theta}$  by updating  $\eta$ , Eqs. (15) to (17).
6:   end for
7:   Add random subset from  $\mathcal{T}_i$  to  $\mathcal{M}$ .
8: end for

```

---

Where the  $p(y) = \alpha_y / \sum_{j=1}^J \alpha_j$ , see [Appendix D.3](#) for the detailed derivation. This objective can then be optimized using gradient based optimization for learning the prototype embedding function  $\mathbf{z} = f(\mathbf{x}; \mathbf{w})$ .

**Predictions.** To make a prediction for a test point  $\mathbf{x}^*$  the class with the maximum (log)-posterior predictive is chosen, where the posterior predictive is:

$$p(y^* = j | \mathbf{x}^*, \mathbf{x}_{1:t}, y_{1:t}) = p(y^* = j | \mathbf{z}^*, \boldsymbol{\theta}_t) = \frac{p(y^* = j, \mathbf{z}^* | \boldsymbol{\theta}_t)}{\sum_i p(y = i, \mathbf{z}^* | \boldsymbol{\theta}_t)}, \quad (19)$$

see [Appendix D.4](#) for further details.

**Preventing forgetting.** As we wish to retain the class prototypes. We make use of coresets: experience from previous tasks. At the end of learning a task  $\mathcal{T}_t$ , we retain subset  $\mathcal{M}_t \subset \mathcal{D}_t$  and augment each new task dataset to ensure that posterior parameters  $\eta_t$  and prototypes are able to retain previous task information.

**Class incremental learning.** In this CL setting we do not tell the CL agent which task it is currently training and evaluating with a task identifier  $\tau$ . So we cannot use the task identifier to select a specific head to use for classifying a test point, or use the task identifier to condition the model in another way (such that  $p(y|\mathbf{x}, \tau)$  where  $\tau$  is the task identifier). Also we require the CL agents to classify each class in the CL benchmarks, for example  $\{0, \dots, 9\}$  for Split-MNIST and Split CIFAR10 and not just  $\{0, 1\}$  for each task as commonly performed (these are called *task-incremental* and *domain-incremental* learning). We believe that these are more realistic and the most important settings to evaluate on.

**Implementation.** For Split-MNIST and Split-FMNIST the baselines and ProtoCL all use two layer NNs with hidden state size of 200. For Split-CIFAR10 and Split-CIFAR100, the baselines and ProtoCL use a four layer convolution neural network with two fully connected layers of size 512 similarly to [Pan et al. \(2020\)](#). For ProtoCL and all baselines which rely on replay we fix the size of the coreset to 200 points per task. For all ProtoCL models we allow the prior Dirichlet parameters to be learned and set their initial value to 0.7 found by a random search over MNIST with ProtoCL. An important hyperparameter for ProtoCL is the embedding dimension of the Gaussian prototypes for Split-MNIST and Split-FMNIST this was set to 128 while for the larger vision datasets this was set to 32 found using grid-search.

Table 1: Mean accuracies across all tasks over CL vision benchmarks for *class incremental learning* ([Van de Ven & Tolias, 2019](#)). All results are averages and standard errors over 10 seeds. \*Uses the predictive entropy to make a decision about which head for class incremental learning.

Method	Coreset	Split-MNIST	Split-FMNIST
VCL ( <a href="#">Nguyen et al., 2017</a> )	✗	$33.01 \pm 0.08$	$32.77 \pm 1.25$
+ coreset	✓	$52.98 \pm 18.56$	$61.12 \pm 16.96$
HIBNN* ( <a href="#">Kessler et al., 2019</a> )	✗	$85.50 \pm 3.20$	$43.70 \pm 20.21$
FROMP ( <a href="#">Pan et al., 2020</a> )	✓	$84.40 \pm 0.00$	$68.54 \pm 0.00$
S-FSVI ( <a href="#">Rudner et al., 2022b</a> )	✓	<b><math>92.94 \pm 0.17</math></b>	$80.55 \pm 0.41$
ProtoCL (ours)	✓	<b><math>93.73 \pm 1.05</math></b>	<b><math>82.73 \pm 1.70</math></b>

Table 2: Mean accuracies across all tasks over CL vision benchmarks for *class incremental learning* (Van de Ven & Tolias, 2019). All results are averages and standard errors over 10 seeds. \*Uses the predictive entropy to make a decision about which head for class incremental learning. Training times have been benchmarked using an Nvidia RTX3090 GPU.

Method	Training time (sec) (↓)	Split CIFAR-10 (acc) (↑)
FROMOP (Pan et al., 2020)	$1425 \pm 28$	$48.92 \pm 10.86$
S-FSVI (Rudner et al., 2022b)	$44434 \pm 91$	$50.85 \pm 3.87$
ProtoCL (ours)	<b><math>384 \pm 6</math></b>	<b><math>55.81 \pm 2.10</math></b>
Split CIFAR-100 (acc)		
S-FSVI (Rudner et al., 2022b)	$37355 \pm 1135$	$20.04 \pm 2.37$
ProtoCL (ours)	<b><math>1425 \pm 28</math></b>	<b><math>23.96 \pm 1.34</math></b>

**Results.** ProtoCL produces good results on CL benchmarks on par or better than S-FSVI (Rudner et al., 2022b) which is state-of-the-art on the smaller CL benchmarks while being a lot more efficient to train and without requiring expensive variational inference. ProtoCL can flexibly scale to larger CL vision benchmarks producing better results than S-FSVI. Code to reproduce all experiments can be found here [anonymous.4open.science/r/bayes\\_cl\\_exploration](https://anonymous.4open.science/r/bayes_cl_exploration). All our experiments are in the more realistic class incremental learning setting, which is a harder setting than those reported in most CL papers, so the results in Table 1 are lower for certain baselines than in the respective papers. We use 200 data points per task, see Figure 12 for a sensitivity analysis of the performance over the Split-MNIST benchmark as a function of core size for ProtoCL.

The stated aim of ProtoCL is not to provide a novel state-of-the-art method for CL, but rather to propose a simple baseline which takes an alternative route than weight-space sequential Bayesian inference. We can achieve strong results that mitigate forgetting, namely by modeling the generative CL process and using sequential Bayesian inference over a few parameters in the class prototype embedding space. We argue that modeling the generative CL process is a fruitful direction for further research rather than attempting sequential Bayesian inference over the weights of a BNN.

## 8 Discussion & Conclusion

In this paper we have revisited the use of sequential Bayesian inference for CL. We can use sequential Bayes to recursively build up the multi-task posterior Eq. (5). Previous methods have relied on approximate inference and see little benefit over SGD. We test the hypothesis of whether this poor performance is due to the approximate inference scheme by using HMC in two simple CL problems. HMC asymptotically samples from the true posterior and we use a density estimator over HMC samples to use as a prior for a new task within the HMC sampling process. This density is multi-modal and accurate with respect to the current task but is not able to improve over using an approximate posterior. This demonstrates just how challenging it is to work with BNN weight posteriors. The source of error comes from the density estimation step. We then look at an analytical example of sequential Bayesian inference where we perform exact inference however due to model misspecification, we observe forgetting. The only way to ensure a well specified model is to assess the multi-task performance over all tasks a priori. This might not be possible in online CL settings. We then model an analytical example over Bayesian NNs and under certain assumptions show that if there is task data imbalances then this will cause forgetting. Because of these results, we argue against performing weight space sequential Bayesian inference and instead model the generative CL problem. We introduce a simple baseline called ProtoCL. ProtoCL doesn’t require complex variational optimization and achieves competitive results to state-of-the-art in the realistic setting of class incremental learning.

This conclusion should not be a surprise since the latest Bayesian CL papers have all relied multi-head architectures or inducing points/coresets to prevent forgetting, rather than better weight-space inference schemes. Our observations are in line with recent theory from (Knoblauch et al., 2020) which states that

---

optimal CL requires perfect memory. Although the results were shown with deterministic NNs the same results follow for BNN with a single set of parameters. Future research directions include enabling coresets of task data to efficiently and accurately approximate the posterior of a BNN to remember previous tasks.

## 9 Acknowledgments

We would like to thank Sebastian Farquhar, Laurence Aitchison, Jeremias Knoblauch and Chris Holmes for discussions. Thanks to Phil Ball for help with writing the paper. SK acknowledges funding from the Oxford-Man Institute of Quantitative Finance. TGJR acknowledges funding from the Rhodes Trust, Qualcomm, and the Engineering and Physical Sciences Research Council (EPSRC). This material is based upon work supported by the United States Air Force and DARPA under Contract No. FA8750-20-C-0002. Any opinions, findings and conclusions or recommendations expressed in this material are those of the author(s) and do not necessarily reflect the views of the United States Air Force and DARPA.

## References

Hongjoon Ahn, Sungmin Cha, Donggyu Lee, and Taesup Moon. Uncertainty-based continual learning with adaptive regularization. *Advances in neural information processing systems*, 32, 2019.

Laurence Aitchison. Bayesian filtering unifies adaptive and non-adaptive neural network optimization methods. *arXiv preprint arXiv:1807.07540*, 2018.

Ari S Benjamin, David Rolnick, and Konrad Kording. Measuring and regularizing networks in function space. *arXiv preprint arXiv:1805.08289*, 2018.

Charles Blundell, Julien Cornebise, Koray Kavukcuoglu, and Daan Wierstra. Weight uncertainty in neural network. In *International Conference on Machine Learning*, pp. 1613–1622. PMLR, 2015.

Pietro Buzzega, Matteo Boschini, Angelo Porrello, Davide Abati, and Simone Calderara. Dark experience for general continual learning: a strong, simple baseline. *Advances in neural information processing systems*, 33:15920–15930, 2020.

Nicolas Chopin, Omiros Papaspiliopoulos, et al. *An introduction to sequential Monte Carlo*, volume 4. Springer, 2020.

Ö Ciftcioglu and E Türkcan. Adaptive training of feedforward neural networks by Kalman filtering. 1995.

Adam D Cobb and Brian Jalaian. Scaling Hamiltonian Monte Carlo Inference for Bayesian Neural Networks with Symmetric Splitting. *Uncertainty in Artificial Intelligence*, 2021.

Matthias De Lange, Rahaf Aljundi, Marc Masana, Sarah Parisot, Xu Jia, Aleš Leonardis, Gregory Slabaugh, and Tinne Tuytelaars. A continual learning survey: Defying forgetting in classification tasks. *IEEE transactions on pattern analysis and machine intelligence*, 44(7):3366–3385, 2021.

Laurent Dinh, Jascha Sohl-Dickstein, and Samy Bengio. Density estimation using real NVP. *arXiv preprint arXiv:1605.08803*, 2016.

Arnaud Doucet, Nando De Freitas, and Neil Gordon. An introduction to sequential Monte Carlo methods. In *Sequential Monte Carlo methods in practice*, pp. 3–14. Springer, 2001.

Sayna Ebrahimi, Mohamed Elhoseiny, Trevor Darrell, and Marcus Rohrbach. Uncertainty-guided continual learning with Bayesian neural networks. *arXiv preprint arXiv:1906.02425*, 2019.

Sebastian Farquhar, Michael A Osborne, and Yarin Gal. Radial bayesian neural networks: Beyond discrete support in large-scale bayesian deep learning. In *International Conference on Artificial Intelligence and Statistics*, pp. 1352–1362. PMLR, 2020.

Robert M French. Catastrophic forgetting in connectionist networks. *Trends in cognitive sciences*, 3(4):128–135, 1999.

---

Alex Graves. Practical variational inference for neural networks. *Advances in neural information processing systems*, 24, 2011.

James Harrison, Apoorva Sharma, Chelsea Finn, and Marco Pavone. Continuous meta-learning without tasks. *arXiv preprint arXiv:1912.08866*, 2019.

Christian Henning, Maria Cervera, Francesco D’Angelo, Johannes Von Oswald, Regina Traber, Benjamin Ehret, Sejin Kobayashi, Benjamin F Grewe, and João Sacramento. Posterior meta-replay for continual learning. *Advances in Neural Information Processing Systems*, 34:14135–14149, 2021.

Yen-Chang Hsu, Yen-Cheng Liu, Anita Ramasamy, and Zsolt Kira. Re-evaluating continual learning scenarios: A categorization and case for strong baselines. *arXiv preprint arXiv:1810.12488*, 2018.

Pavel Izmailov, Sharad Vikram, Matthew D Hoffman, and Andrew Gordon Wilson. What Are Bayesian Neural Network Posteriors Really Like? *arXiv preprint arXiv:2104.14421*, 2021.

Arthur Jacot, Franck Gabriel, and Clément Hongler. Neural tangent kernel: Convergence and generalization in neural networks. *arXiv preprint arXiv:1806.07572*, 2018.

Rudolph Emil Kalman. A new approach to linear filtering and prediction problems. 1960.

Sanyam Kapoor, Theofanis Karaletsos, and Thang D Bui. Variational auto-regressive Gaussian processes for continual learning. In *International Conference on Machine Learning*, pp. 5290–5300. PMLR, 2021.

Samuel Kessler, Vu Nguyen, Stefan Zohren, and Stephen Roberts. Hierarchical Indian buffet neural networks for Bayesian continual learning. *arXiv preprint arXiv:1912.02290*, 2019.

James Kirkpatrick, Razvan Pascanu, Neil Rabinowitz, Joel Veness, Guillaume Desjardins, Andrei A. Rusu, Kieran Milan, John Quan, Tiago Ramalho, Agnieszka Grabska-Barwinska, Demis Hassabis, Claudia Clopath, Dharshan Kumaran, and Raia Hadsell. Overcoming catastrophic forgetting in neural networks. *Proceedings of the National Academy of Sciences*, 114(13):3521–3526, 2017. ISSN 0027-8424. doi: 10.1073/pnas.1611835114.

Jeremias Knoblauch, Hisham Husain, and Tom Diethe. Optimal continual learning has perfect memory and is NP-hard. In *International Conference on Machine Learning*, pp. 5327–5337. PMLR, 2020.

Abhishek Kumar, Sunabha Chatterjee, and Piyush Rai. Bayesian structural adaptation for continual learning. In *International Conference on Machine Learning*, pp. 5850–5860. PMLR, 2021.

Yann LeCun, Léon Bottou, Yoshua Bengio, and Patrick Haffner. Gradient-based learning applied to document recognition. *Proceedings of the IEEE*, 86(11):2278–2324, 1998.

Noel Loo, Siddharth Swaroop, and Richard E Turner. Generalized variational continual learning. *arXiv preprint arXiv:2011.12328*, 2020.

David JC MacKay. A practical Bayesian framework for backpropagation networks. *Neural computation*, 4(3): 448–472, 1992.

Nikhil Mehta, Kevin Liang, Vinay Kumar Verma, and Lawrence Carin. Continual learning using a bayesian nonparametric dictionary of weight factors. In *International Conference on Artificial Intelligence and Statistics*, pp. 100–108. PMLR, 2021.

Radford M Neal et al. MCMC using Hamiltonian dynamics. *Handbook of Markov chain Monte Carlo*, 2(11): 2, 2011.

Cuong V Nguyen, Yingzhen Li, Thang D Bui, and Richard E Turner. Variational continual learning. *arXiv preprint arXiv:1710.10628*, 2017.

Pingbo Pan, Siddharth Swaroop, Alexander Immer, Runa Eschenhagen, Richard E Turner, and Mohammad Emtiyaz Khan. Continual deep learning by functional regularisation of memorable past. *arXiv preprint arXiv:2004.14070*, 2020.

---

Kaare Brandt Petersen, Michael Syskind Pedersen, et al. The matrix cookbook. *Technical University of Denmark*, 7(15):510, 2008.

Sylvestre-Alvise Rebuffi, Alexander Kolesnikov, Georg Sperl, and Christoph H Lampert. ICARL: Incremental classifier and representation learning. In *Proceedings of the IEEE conference on Computer Vision and Pattern Recognition*, pp. 2001–2010, 2017.

Hippolyt Ritter, Aleksandar Botev, and David Barber. Online structured Laplace approximations for overcoming catastrophic forgetting. *arXiv preprint arXiv:1805.07810*, 2018.

Tim G. J. Rudner, Zonghao Chen, Yee Whye Teh, and Yarin Gal. Tractable Function-Space Variational Inference in Bayesian Neural Networks. 2022a.

Tim G. J. Rudner, Freddie Bickford Smith, Qixuan Feng, Yee Whye Teh, and Yarin Gal. Continual Learning via Sequential Function-Space Variational Inference. In *Proceedings of the 38th International Conference on Machine Learning*, Proceedings of Machine Learning Research. PMLR, 2022b.

Jonathan Schwarz, Wojciech Czarnecki, Jelena Luketina, Agnieszka Grabska-Barwinska, Yee Whye Teh, Razvan Pascanu, and Raia Hadsell. Progress & compress: A scalable framework for continual learning. In *International Conference on Machine Learning*, pp. 4528–4537. PMLR, 2018.

Jake Snell, Kevin Swersky, and Richard S Zemel. Prototypical networks for few-shot learning. *arXiv preprint arXiv:1703.05175*, 2017.

Siddharth Swaroop, Cuong V Nguyen, Thang D Bui, and Richard E Turner. Improving and understanding variational continual learning. *arXiv preprint arXiv:1905.02099*, 2019.

Sebastian Thrun and Tom M Mitchell. Lifelong robot learning. *Robotics and autonomous systems*, 15(1-2): 25–46, 1995.

Michalis K Titsias, Jonathan Schwarz, Alexander G de G Matthews, Razvan Pascanu, and Yee Whye Teh. Functional regularisation for continual learning with Gaussian processes. *arXiv preprint arXiv:1901.11356*, 2019.

Gido M Van de Ven and Andreas S Tolias. Three scenarios for continual learning. *arXiv preprint arXiv:1904.07734*, 2019.

Andrew G Wilson and Pavel Izmailov. Bayesian deep learning and a probabilistic perspective of generalization. *Advances in neural information processing systems*, 33:4697–4708, 2020.

Chen Zeno, Itay Golan, Elad Hoffer, and Daniel Soudry. Task agnostic continual learning using online variational bayes. *arXiv preprint arXiv:1803.10123*, 2018.

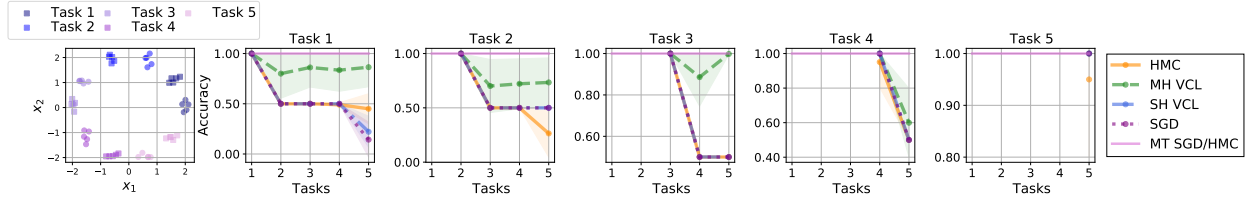


Figure 7: Continual learning binary classification accuracies from the toy Gaussian dataset similar to (Henning et al., 2021) using 10 random seeds. The pink solid line is a multi-task (MT) baseline test accuracy using SGD/HMC.

## Supplementary Material

### A The Toy Gaussians Dataset

See Fig. 7 for a visualization of the toy Gaussians dataset which we use as a simple CL problem. This is used for evaluating our method for propagating the true posterior by using HMC for posterior inference and then using a density estimator on HMC samples as a prior for a new task. We construct 5, 2-way classification problems for CL. Each 2-way task involves classifying adjacent circles and squares Fig. 7. With a 2 layer network with 10 neurons we get a test accuracy of 1.0 for the multi-task learning of all 5 tasks together. Hence according to Eq. (3) a BNN with the same size should be able to learn all 5 binary classification tasks continually by sequentially building up the posterior.

### B HMC implementation details

We set the prior for  $\mathcal{T}_1$ , to  $p_1(\boldsymbol{\theta}) = \mathcal{N}(0, \tau^{-1}\mathbb{I})$  with  $\tau = 10$ . We burn-in the HMC chain for 1000 steps and sample for 10000 more steps and run 20 different chains to obtain samples from our posterior, which we then pass to our density estimator. We use a step size of 0.001 and trajectory length of  $L = 20$ , see Appendix C for further implementation details of the density estimation procedure. For the GMM we optimize for the number of components by using a holdout set of HMC samples.

### C Density Estimation Diagnostics

We provide plots to show that the HMC chains indeed sample from the posterior have converged in Figure 9 and Figure 11. We run 20 HMC sampling chains and randomly select one chain to plot for each seed (of 10). We run HMC over 10 seeds and aggregate the results Figure 3 and Figure 7. The posteriors  $p(\boldsymbol{\theta}|\mathcal{D}_1), \dots$  are approximated with a GMM and used as a prior for the second task and so forth.

We provide empirical evidence to show that the density estimators have fit to HMC samples of the posterior in Figure 8 and Figure 10. Where we show the number of components of the GMM density estimator which we use as a prior for a new task are all multi-modal posteriors. We show the BNN accuracy when sampling BNN weights from our GMM all recover the accuracy of the converged HMC samples. The effective sample size (ESS) of the 20 chains which is a measure of how correlated the samples are (higher is better). The reported ESS values for our experiments are in line with previous work which uses HMC for BNN inference (Cobb & Jalaian, 2021).

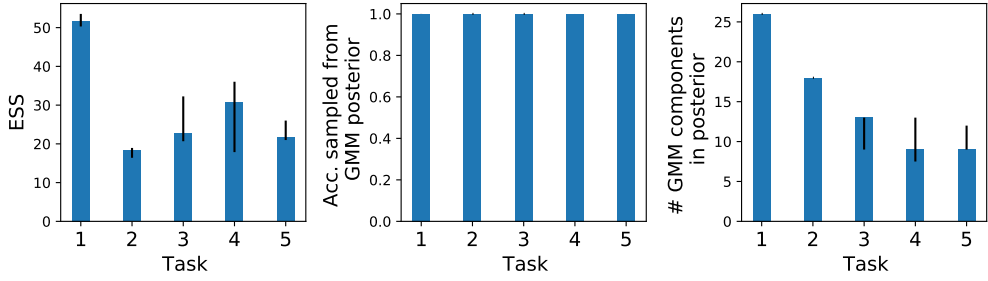


Figure 8: Diagnostics from using a GMM prior fit to samples of the posterior generated from HMC, all results are for 10 random seeds. **Left**, effective sample sizes (ESS) of the resulting HMC chains of the posterior, all are greater than those reported in other works using HMC for BNNs (Cobb & Jalaian, 2021). **Middle**, the accuracy of the BNN when using samples from the GMM density estimator instead from the samples from HMC. **Right**, The optimal number of components of each GMM posterior fitted with a holdout set of HMC samples by maximizing the likelihood.

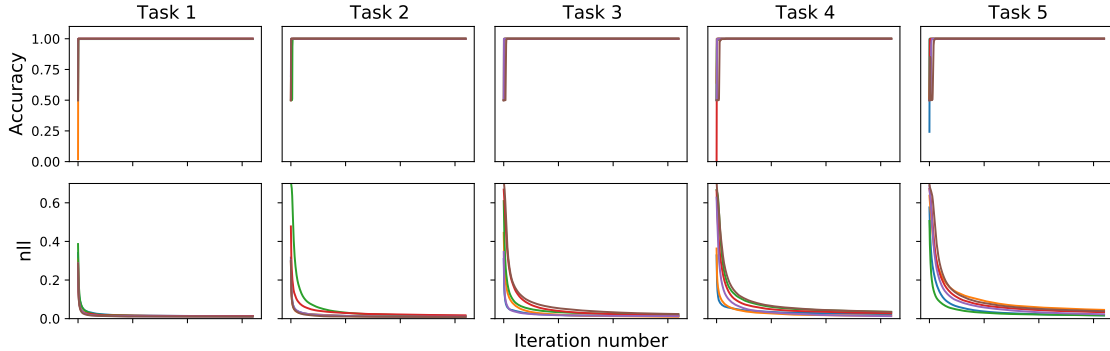


Figure 9: Convergence plots from a one randomly sampled HMC chain (of 20) for each task over 10 different runs (seeds) for 5 tasks from the toy Gaussians dataset similar to Henning et al. (2021) (visualized in Fig. 7). We use a GMM density estimator as the prior conditioned on previous task data.

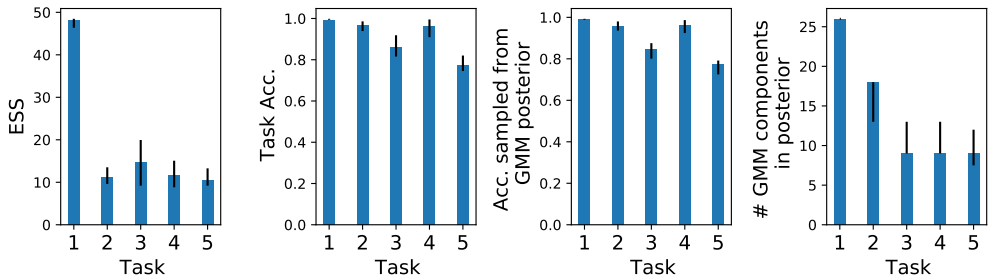


Figure 10: Diagnostics from using a GMM to fit samples of the posterior HMC samples, all results are for 10 random seeds on the toy dataset from Pan et al. (2020) (and visualized in Fig. 3). **Left**, effective sample sizes (ESS) of the resulting HMC chains of the posterior, all are greater than those reported in other works using HMC for BNNs (Cobb & Jalaian, 2021). **Middle left**, the current task accuracy from HMC sampling. **Middle right**, the accuracy of the BNN when using samples from the GMM density estimator instead of the converged HMC samples. **Right**, The optimal number of components of each GMM posterior fitted with a holdout set of HMC samples by maximizing the likelihood.

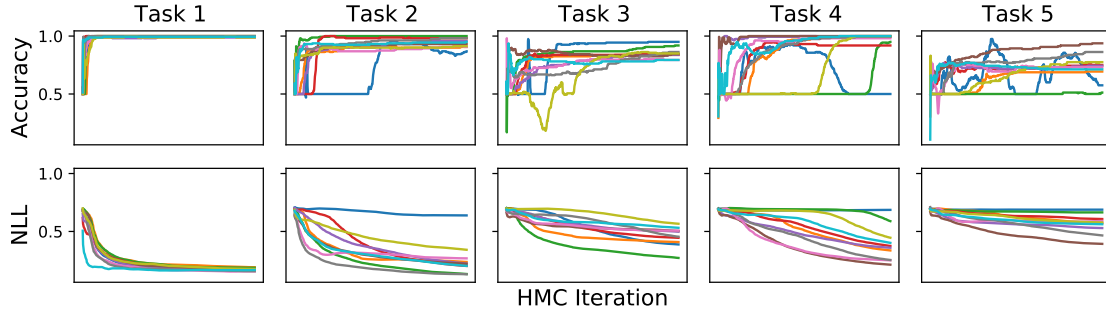


Figure 11: Convergence plots from a randomly sampled HMC chain (of 20) for each task over 10 different seeds for 5 tasks from the toy dataset from (Pan et al., 2020) (see Fig. 3 for a visualization of the data). We use a GMM density estimator as a prior.

## D Prototypical Bayesian Continual Learning

ProtoCL models the generative process of CL where new tasks are comprised of new classes  $j \in \{1, \dots, J\}$  of a total of  $J$  and can be modeled by using a categorical distribution with a Dirichlet prior:

$$y_{i,t} \sim \text{Cat}(p_{1:J}), \quad p_{1:J} \sim \text{Dir}(\alpha_t). \quad (\text{D.1})$$

We learn a joint embedding space for our data with a NN,  $\mathbf{z} = f(\mathbf{x}; \mathbf{w})$  with parameters  $\mathbf{w}$ . The embedding space for each class is Gaussian whose mean has a prior which is also Gaussian:

$$\mathbf{z}_{it} | y_{it} \sim \mathcal{N}(\bar{\mathbf{z}}_{yt}, \Sigma_\epsilon), \quad \bar{\mathbf{z}}_{yt} \sim \mathcal{N}(\boldsymbol{\mu}_{yt}, \Lambda_{yt}^{-1}). \quad (\text{D.2})$$

By ensuring that we have an embedding per class and using a memory of past data, we ensure that the embedding does not drift. The posterior parameters are  $\eta_t = \{\alpha_t, \boldsymbol{\mu}_{1:J,t}, \Lambda_{1:J,t}^{-1}\}$ .

### D.1 Inference

As the Dirichlet prior is conjugate with the Categorical distribution and so is the Gaussian distribution with a Gaussian prior over the mean of the embedding, then we can calculate posteriors in closed form and update our parameters as we see new data online without using gradient based updates. We perform gradient based learning of the NN embedding function  $f(\cdot; \mathbf{w})$  with parameters  $\mathbf{w}$ . We optimize the model by maximizing the log-predictive posterior of the data and use the softmax over class probabilities to perform predictions. The posterior over class probabilities  $\{p_j\}_{j=1}^J$  and class embeddings  $\{\bar{\mathbf{z}}_{y_j}\}_{j=1}^J$  is denoted as  $p(\theta)$  for short hand and has parameters are  $\eta_t = \{\alpha_t, \boldsymbol{\mu}_{1:J,t}, \Lambda_{1:J,t}^{-1}\}$  are updated in closed form at each iteration of gradient descent.

### D.2 Sequential updates

We can obtain our posterior:

$$p(\boldsymbol{\theta}_t | \mathcal{D}_t) \propto p(\mathcal{D}_t | \boldsymbol{\theta}_t) p(\boldsymbol{\theta}_t) \quad (\text{D.3})$$

$$= \prod_{i=1}^{N_t} p(\mathbf{z}_t^i | y_t^i; \bar{\mathbf{z}}_{yt}, \Sigma_{\epsilon,y_t}) p(y_t^i | p_{1:J}) p(p_{1:J}; \alpha_t) p(\bar{\mathbf{z}}_{yt}; \boldsymbol{\mu}_{yt,t}, \Lambda_{yt,t}^{-1}) \quad (\text{D.4})$$

$$= \mathcal{N}(\boldsymbol{\mu}_{t+1}, \Sigma_{t+1}) \text{Dir}(\alpha_{t+1}), \quad (\text{D.5})$$

where  $N_t$  is the number of data points seen during update  $t$ . Concentrating on the Categorical-Dirichlet conjugacy:

$$\text{Dir}(\alpha_{t+1}) \propto p(p_{1:J}; \alpha_t) \prod_{i=1}^{N_t} p(y_t^i; p_{i:J}) \quad (\text{D.6})$$

$$\propto \prod_{j=1}^J p_j^{\alpha_j-1} \prod_{i=1}^{N_t} \prod_{j=1}^J p_j^{\mathbb{I}(y_t^i=j)} \quad (\text{D.7})$$

$$= \prod_{j=1}^J p_j^{\alpha_j-1 + \sum_{i=1}^{N_t} \mathbb{I}(y_t^i=j)}. \quad (\text{D.8})$$

Thus:

$$\alpha_{t+1,j} = \alpha_{t,j} + \sum_{i=1}^{N_t} \mathbb{I}(y_t^i=j). \quad (\text{D.9})$$

Also, due to Gaussian-Gaussian conjugacy, then the posterior for the Gaussian prototype of the embedding for each class is:

$$\mathcal{N}(\boldsymbol{\mu}_{t+1}, \Lambda_{t+1}) \propto \prod_{i=1}^{N_t} \mathcal{N}(\mathbf{z}_t^i | y_t^i; \bar{\mathbf{z}}_{y_t}, \Sigma_\epsilon) \mathcal{N}(\bar{\mathbf{z}}_{y_t}; \boldsymbol{\mu}_{y_t, t}, \Lambda_{y_t}^{-1}) \quad (\text{D.10})$$

$$= \prod_{y_t \in \{1, \dots, J\}} \mathcal{N}(\mathbf{z}_{y_t} | y_t; \bar{\mathbf{z}}_{y_t}, \frac{1}{N_{y_t}} \Sigma_\epsilon) \mathcal{N}(\bar{\mathbf{z}}_{y_t}; \boldsymbol{\mu}_{y_t, t}, \Lambda_{y_t}^{-1}) \quad (\text{D.11})$$

$$= \prod_{y_t \in \{1, \dots, J\}} \mathcal{N}(\bar{\mathbf{z}}_{y_t}; \boldsymbol{\mu}_{t+1}, \Lambda_{y_t}^{-1}), \quad (\text{D.12})$$

where  $N_{y_t}$  is the number of points of class  $y_t$  from the set of all classes  $C = \{1, \dots, J\}$ . The update equations for the mean and variance of the posterior are:

$$\Lambda_{y_{t+1}} = \Lambda_{y_t} + N_{y_t} \Sigma_\epsilon^{-1}, \quad \forall y_t \in C_t \quad (\text{D.13})$$

$$\Lambda_{y_{t+1}} \boldsymbol{\mu}_{y_{t+1}} = N_{y_t} \Sigma_\epsilon^{-1} \bar{\mathbf{z}}_{y_t} + \Lambda_{y_t} \boldsymbol{\mu}_{y_t}, \quad \forall y_t \in C_t. \quad (\text{D.14})$$

### D.3 ProtoCL Objective

The posterior predictive distribution we want to optimize is:

$$p(\mathbf{z}, y) = \int p(\mathbf{z}, y | \boldsymbol{\theta}; \eta) p(\boldsymbol{\theta}; \eta) d\boldsymbol{\theta}, \quad (\text{D.15})$$

where  $p(\boldsymbol{\theta})$  denotes the distributions over class probabilities  $\{p_j\}_{j=1}^J$  and mean embeddings  $\{\bar{\mathbf{z}}_{y_j}\}_{j=1}^J$ ,

$$p(\mathbf{z}, y) = \int \prod_{i=1}^{N_t} p(\mathbf{z}_{it} | y_{it}; \bar{\mathbf{z}}_{y_t}, \Sigma_\epsilon) p(y_{it} | p_{1:J}) p(p_{1:J}; \alpha_t) p(\bar{\mathbf{z}}_{y_t}; \boldsymbol{\mu}_{y_t, t}, \Lambda_{y_t}^{-1}) dp_{1:J} d\bar{\mathbf{z}}_{y_t} \quad (\text{D.16})$$

$$= \int \prod_{i=1}^{N_t} p(\mathbf{z}_{it} | y_{it}; \bar{\mathbf{z}}_{y_t}, \Sigma_\epsilon) p(\bar{\mathbf{z}}_{y_t}; \boldsymbol{\mu}_{y_t, t}, \Lambda_{y_t}^{-1}) d\bar{\mathbf{z}}_{y_t} \underbrace{\int \prod_{i=1}^{N_t} p(y_{it} | p_{1:J}) p(p_{1:J}; \alpha_t) dp_{1:J}}_{\prod_i p(y_i) = p(y)} \quad (\text{D.17})$$

$$= p(y) \prod_{i=1}^{N_t} Z_i^{-1} \int \mathcal{N}(\bar{\mathbf{z}}_{y_{it}}; \mathbf{c}, C) d\bar{\mathbf{z}}_{y_t} \quad (\text{D.18})$$

$$= p(y) \prod_{i=1}^{N_t} \mathcal{N}(\mathbf{z}_{it} | y_{it}; \boldsymbol{\mu}_{y_t, t}, \Sigma_\epsilon + \Lambda_{y_t, t}^{-1}). \quad (\text{D.19})$$

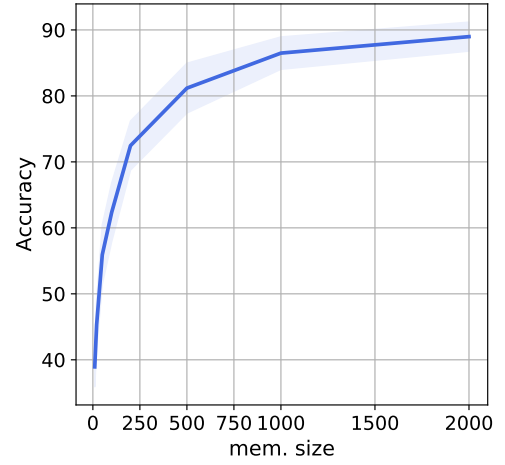


Figure 12: Split-MNIST average test accuracy over all 5 tasks for different memory sizes. Accuracies are over 10 seeds.

Where in Eq. (D.18) we use §8.1.8 in (Petersen et al., 2008). The term  $p(y)$  is:

$$p(y) = \int p(y|p_{1:J})p(p_{1:J}; \alpha_t)dp_{1:J} \quad (\text{D.20})$$

$$= \int p_y \frac{\Gamma(\sum_{j=1}^J \alpha_j)}{\prod_{j=1}^J \Gamma(\alpha_j)} \prod_{j=1}^J p_j^{\alpha_j-1} dp_{1:J} \quad (\text{D.21})$$

$$= \frac{\Gamma(\sum_{j=1}^J \alpha_j)}{\prod_{j=1}^J \Gamma(\alpha_j)} \int \prod_{j=1}^J p_j^{\mathbb{I}(y=j)+\alpha_j-1} dp_{1:J} \quad (\text{D.22})$$

$$= \frac{\Gamma(\sum_{j=1}^J \alpha_j)}{\prod_{j=1}^J \Gamma(\alpha_j)} \frac{\prod_{j=1}^J \Gamma(\mathbb{I}(y=j) + \alpha_j)}{\Gamma(1 + \sum_{j=1}^J \alpha_j)} \quad (\text{D.23})$$

$$= \frac{\Gamma(\sum_{j=1}^J \alpha_j)}{\prod_{j=1}^J \Gamma(\alpha_j)} \frac{\prod_{j=1}^J \Gamma(\mathbb{I}(y=j) + \alpha_j)}{\sum_{j=1}^J \alpha_j \Gamma(\sum_{j=1}^J \alpha_j)} \quad (\text{D.24})$$

$$= \frac{\prod_{j=1, j \neq y}^J \Gamma(\alpha_j)}{\prod_{j=1}^J \Gamma(\alpha_j)} \frac{\Gamma(1 + \alpha_y)}{\sum_{j=1}^J \alpha_j} \quad (\text{D.25})$$

$$= \frac{\prod_{j=1, j \neq y}^J \Gamma(\alpha_j)}{\prod_{j=1}^J \Gamma(\alpha_j)} \frac{\alpha_y \Gamma(\alpha_y)}{\sum_{j=1}^J \alpha_j} \quad (\text{D.26})$$

$$(\text{D.27})$$

where we use the identity  $\Gamma(n+1) = n\Gamma(n)$ .

#### D.4 Predictions

To make a prediction for a test point  $\mathbf{x}^*$ :

$$p(y^* = j | \mathbf{x}^*, \mathbf{x}_{1:t}, y_{1:t}) = p(y^* = j | \mathbf{z}^*, \boldsymbol{\theta}_t) \quad (\text{D.28})$$

$$= \frac{p(\mathbf{z}^* | y^* = j, \boldsymbol{\theta}_t) p(y^* = j | \boldsymbol{\theta}_t)}{\sum_i p(\mathbf{z}^* | y^* = i, \eta_t) p(y^* = i | \boldsymbol{\theta}_t)} \quad (\text{D.29})$$

$$= \frac{p(y^* = j, \mathbf{z}^* | \boldsymbol{\theta}_t)}{\sum_i p(y^* = i, \mathbf{z}^* | \boldsymbol{\theta}_t)}, \quad (\text{D.30})$$

where  $\boldsymbol{\theta}_t$  are sufficient statistics for  $(\mathbf{x}_{1:t}, y_{1:t})$ .

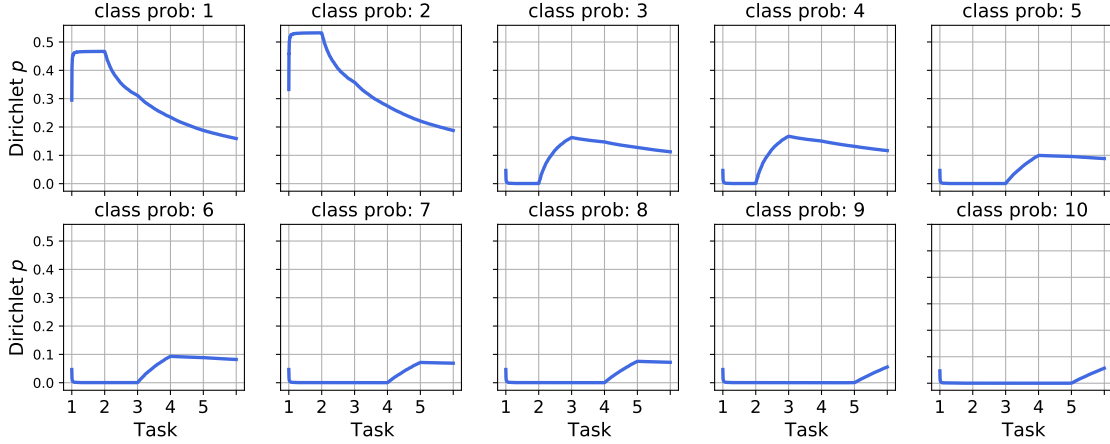


Figure 13: The evolution of the Dirichlet parameters  $\alpha_t$  for each class in Split-MNIST tasks for ProtoCL. All  $\alpha_j$  are shown over 10 seeds with  $\pm 1$  standard error. By the end of training all classes are roughly equally likely, as we have trained on equal amounts of all classes.

**Preventing forgetting.** As we wish to retain the task specific prototypes, at the end of learning a task  $\mathcal{T}_t$  we take a small subset of the data as a memory to ensure that posterior parameters and prototypes do not drift, see [Algorithm 1](#).

## D.5 Experimental Setup

The prototype variance,  $\Sigma_\epsilon$  is set to a diagonal matrix with the variances of each prototype set to 0.05. The prototype prior precisions,  $\Lambda_{yt}$  are also diagonals and initialized randomly and exponentiated to ensure a positive semi-definite covariance for the sequential updates. The parameters  $\alpha_j \forall j$  are set to 0.78 which was found by random search over the validation set on MNIST. We also allow  $\alpha_j$  to be learned in the gradient update step in addition to the sequential update step (lines 4 and 5 [Algorithm 1](#)), see [Fig. 13](#) to see the evolution of the  $\alpha_j$  or all classes  $j$  over the course of learning Split-MNIST.

For the Split-MNIST and Split-FMNIST benchmarks we use a NN with 2 layers of size 200 and trained for 50 epochs with an Adam optimizer. We perform a grid-search over learning rates, dropout rates and weight decay coefficients. The embedding dimension is set to 128. For the Split-CIFAR10 and Split-CIFAR100 benchmarks, we use the same network as [Pan et al. \(2020\)](#) which consists of 4 convolution layers and 2 linear layers. We train the networks for 80 epochs for each task with the Adam optimizer with a learning rate of  $1e - 3$ . The embedding dimension is set to 32. All experiments are run a single GPU NVIDIA RTX 3090.

## E Sequential Bayesian Estimation as Bayesian Neural Network optimization

We shall consider inference in the graphical model depicted in [Fig. 14](#). The aim is to infer the optimal BNN weights,  $\theta_t^*$  at time  $t$  given observations and the previous BNN weights. We assume a Gaussian posterior over weights with full covariance hence we model interactions between all weights. We shall consider the online setting where we see one data point  $(\mathbf{x}_t, y_t)$  at a time and we will make no assumption as to whether the data comes from the same task or different tasks over the course of learning.

We set up the problem of sequential Bayesian inference as a filtering problem and we leverage the work of [Aitchison \(2018\)](#) which casts NN optimization as Bayesian sequential inference. We make the reasonable assumption that the distribution over weights is a Gaussian with full covariance. Since reasoning about the full covariance matrix of a BNN is intractable we instead consider the  $i$ -th parameter and reason about the dynamics of the optimal estimates  $\theta_{it}^*$  as a function of all the other parameters  $\theta_{-it}$ . Each weight is functionally dependent on all others. If we had access to the full covariance of the parameters then we could reason about the unknown optimal weights  $\theta_{it}^*$  given the values of all the other weights  $\theta_{-it}$ . However, since

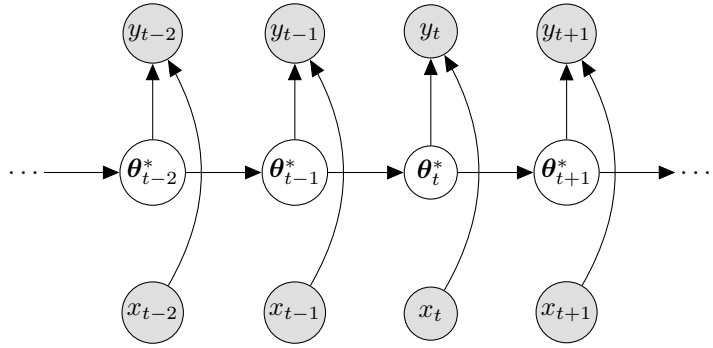


Figure 14: Graphical model of under which we perform inference in Section 5. Grey nodes are observed and white are latent variables.

we do not have access to the full covariance another approach is to reason about the dynamics of  $\theta_{it}^*$  given the dynamics of  $\theta_{-it}$  and assume that the values of the weights are close to those of the previous time-step (Jacot et al., 2018) and so we cast the problem as a dynamical system.

Consider a quadratic loss of the form:

$$\mathcal{L}(\mathbf{x}_t, y_t; \boldsymbol{\theta}) = \mathcal{L}_t(\boldsymbol{\theta}) = -\frac{1}{2} \boldsymbol{\theta}^\top \mathbf{H} \boldsymbol{\theta} + \mathbf{z}_t^\top \boldsymbol{\theta}, \quad (\text{E.31})$$

which we can arrive by simple Taylor expansion where  $\mathbf{H}$  is the Hessian which is assumed to constant across data points but not across the parameters  $\boldsymbol{\theta}$ . If the BNN output takes the form  $f(\mathbf{x}_t; \boldsymbol{\theta})$ , then the derivative evaluated at  $\boldsymbol{\theta}_t$  is  $\mathbf{z}_t = \frac{\partial \mathcal{L}(\mathbf{x}_t, y_t; \boldsymbol{\theta})}{\partial \boldsymbol{\theta}}|_{\boldsymbol{\theta}=\boldsymbol{\theta}_t}$ . To construct the dynamical equations for our weights, consider the gradient for a single datapoint:

$$\frac{\partial \mathcal{L}_t(\boldsymbol{\theta})}{\partial \boldsymbol{\theta}} = -\mathbf{H} \boldsymbol{\theta} + \mathbf{z}_t. \quad (\text{E.32})$$

If we consider the gradient for the  $i$ -th weight while all other parameters are set to their current estimate:

$$\frac{\partial \mathcal{L}(\theta_i, \boldsymbol{\theta}_{-i})}{\partial \theta_i} = -H_{ii}\theta_{it} - \mathbf{H}_{-ii}^\top \boldsymbol{\theta}_{-it} + z_{ti}. \quad (\text{E.33})$$

When the gradient is set to zero we recover the optimal value for  $\theta_{it}$ , denoted as  $\theta_{it}^*$ :

$$\theta_{it}^* = -\frac{1}{H_{ii}} \mathbf{H}_{-ii}^\top \boldsymbol{\theta}_{-it}. \quad (\text{E.34})$$

since  $z_{ti} = 0$  at the modes. The equation above shows us that the dynamics of the optimal weight  $\theta_{it}^*$  is dependent on all the other current values of the parameters  $\boldsymbol{\theta}_{-it}$ . That is, the dynamics of  $\theta_{it}^*$  will be governed by the dynamics of the weights  $\boldsymbol{\theta}_{-it}$ . The dynamics of  $\boldsymbol{\theta}_{-it}$  will be a complex stochastic process dependent on many different variables. Since reasoning about the dynamics is intractable we instead assume a discretized Ornstein-Uhlenbeck process for the weights  $\boldsymbol{\theta}_{-it}$  with reversion speed  $\vartheta \in \mathbb{R}_+$  and noise variance  $\eta_{-i}^2$ :

$$p(\boldsymbol{\theta}_{-i,t+1} | \boldsymbol{\theta}_{-i,t}) = \mathcal{N}((1 - \vartheta)\boldsymbol{\theta}_{-i,t}, \eta_{-i}^2), \quad (\text{E.35})$$

this implies that the dynamics for the optimal weight is defined by

$$p(\theta_{i,t+1}^* | \theta_{i,t}^*) = \mathcal{N}((1 - \vartheta)\theta_{i,t}^*, \eta^2), \quad (\text{E.36})$$

where  $\eta^2 = \eta_{-i}^2 \mathbf{H}_{-ii}^\top \mathbf{H}_{-ii}$ . This same assumption is made in Aitchison (2018). This assumes a parsimonious model of the dynamics. Together with our likelihood:

$$p(y_t | \mathbf{x}_t; \boldsymbol{\theta}_t^*) = \mathcal{N}(y_t; f(\mathbf{x}_t; \boldsymbol{\theta}_t^*), \sigma^2) \quad (\text{E.37})$$

where  $f(\cdot, \boldsymbol{\theta})$  is a neural network prediction with weights  $\boldsymbol{\theta}$ , we can now define a linear dynamical system for the optimal weight  $\theta_i^*$  by linearizing the the Bayesian NN (Jacot et al., 2018) and by using the transition dynamics in Eq. (E.36). Thus we are able to infer the posterior distribution over the optimal weights using Kalman filter like updates (Kalman, 1960). As the dynamics and likelihood are Gaussian, then the prior and posterior are also Gaussian, for ease of notation we drop the index  $i$  such that  $\theta_{it}^* = \theta_t^*$ :

$$p(\theta_t^* | (\mathbf{x}, y)_{t-1}, \dots, (\mathbf{x}, y)_1) = \mathcal{N}(\mu_{t,\text{prior}}, \sigma_{t,\text{prior}}^2) \quad (\text{E.38})$$

$$p(\theta_t^* | (\mathbf{x}, y)_t, \dots, (\mathbf{x}, y)_1) = \mathcal{N}(\mu_{t,\text{post}}, \sigma_{t,\text{post}}^2) \quad (\text{E.39})$$

By using the transition dynamics and the prior we can obtain closed form updates:

$$p(\theta_t^* | (\mathbf{x}, y)_{t-1}, \dots, (\mathbf{x}, y)_1) = \int p(\theta_t^* | \theta_{t-1}^*) p(\theta_{t-1}^* | (\mathbf{x}, y)_{t-1}, \dots, (\mathbf{x}, y)_1) d\theta_{t-1}^* \quad (\text{E.40})$$

$$\mathcal{N}(\theta_t^*; \mu_{t,\text{prior}}, \sigma_{t,\text{prior}}^2) = \int \mathcal{N}(\theta_t^*; (1 - \vartheta)\theta_{t-1}^*, \eta^2) \mathcal{N}(\theta_{t-1}^*; \mu_{t-1,\text{post}}, \sigma_{t-1,\text{post}}^2) d\theta_{t-1}^*. \quad (\text{E.41})$$

Integrating out  $\theta_{t-1}^*$  we can get updates for the prior for the next timestep as follows:

$$\mu_{t,\text{prior}} = (1 - \vartheta)\mu_{t-1,\text{post}} \quad (\text{E.42})$$

$$\sigma_{t,\text{prior}}^2 = \eta^2 + (1 - \vartheta)^{-2}\sigma_{t-1,\text{post}}^2. \quad (\text{E.43})$$

The updates for obtaining our posterior parameters:  $\mu_{t,\text{post}}$  and  $\sigma_{t,\text{post}}^2$ , comes from applying Bayes' theorem:

$$\log \mathcal{N}(\theta_t^*; \mu_{t,\text{post}}, \sigma_{t,\text{post}}^2) \propto \log \mathcal{N}(y_t; f(\mathbf{x}_t; \theta_t^*), \sigma^2) + \log \mathcal{N}(\theta_t^*; \mu_{t,\text{prior}}, \sigma_{t,\text{prior}}^2), \quad (\text{E.44})$$

by linearizing our Bayesian NN such that  $f(\mathbf{x}_t, \theta_0) \approx f(\mathbf{x}_t, \theta_0) + \frac{\partial f(\mathbf{x}_t; \theta_t^*)}{\partial \theta_t^*}(\theta_t^* - \theta_0)$  and by substituting into Eq. (E.44) we obtain our update equation for the posterior of the mean of our BNN parameters:

$$-\frac{1}{2\sigma_{t,\text{post}}^2}(\theta_t^* - \mu_{t,\text{post}})^2 = -\frac{1}{2\sigma^2}(y - g(\mathbf{x}_t)\theta_t^*)^2 - \frac{1}{2\sigma_{t,\text{prior}}^2}(\theta_t^* - \mu_{t,\text{prior}})^2 \quad (\text{E.45})$$

$$\mu_{t,\text{post}} = \sigma_{t,\text{post}}^2 \left( \frac{\mu_{t,\text{prior}}}{\sigma_{t,\text{prior}}^2} + \frac{y}{\sigma^2} g(\mathbf{x}_t) \right), \quad (\text{E.46})$$

where  $g(\mathbf{x}_t) = \frac{\partial f(\mathbf{x}_t; \theta_t^*)}{\partial \theta_t^*}$ , and the update equation for the variance of the Gaussian posterior is:

$$\frac{1}{\sigma_{t,\text{post}}^2} = \frac{g(\mathbf{x}_t)^2}{\sigma^2} + \frac{1}{\sigma_{t,\text{prior}}^2}. \quad (\text{E.47})$$

From our update equations Eq. (E.46) and Eq. (E.47) we can notice that the posterior mean depends linearly on the prior and an additional data dependent term. These equations are similar to the filtering example in Section 4. So under certain assumptions above, a BNN should behave similarly. If there exists a task data imbalance then the data term will dominate the prior term in Eq. (E.46) and could lead to forgetting of previous tasks.